*International Immunology, Vol. 17, No. 8, pp. 993–1007*
doi:10.1093/intimm/dxh281



# Asthmatic changes in mice lacking T-bet are mediated by IL-13

**Susetta Finotto[1], Michael Hausding[1], Aysefa Doganci[1], Joachim H. Maxeiner[1], Hans A. Lehr[2], Cornelia Luft[1], Peter R. Galle[1]** and **Laurie H. Glimcher[3,4]**

[1]Laboratory of Cellular and Molecular Immunology of the Lung and [2]Pathology Department, University of Mainz, Mainz, Germany
[3]Department of Immunology and Infections Diseases, Harvard School of Public Health and [4]Department of Medicine, Harvard Medical School, Boston, MA, USA

*Keywords*: airway remodeling, asthma, cytokines, T-bet, TGF-β

### Abstract

**Mice with a targeted deletion of the T-bet gene exhibit spontaneous airway hyperresponsiveness (AHR), airway inflammation, enhanced recovery of $T_h2$ cytokines from bronchoalveolar lavage fluid, sub-epithelial collagen deposition and myofibroblast transformation. Here we analyze the mechanisms responsible for the chronic airway remodeling observed in these mice. CD4+ T cells isolated from the lung of T-bet-deficient mice were spontaneously activated $CD44^{high}CD69^{high}$ memory T cells, with a typical $T_h2$ cytokine profile. Neutralization of IL-13 but not IL-4 resulted in amelioration of AHR in airways of mice lacking T-bet. IL-13 blockade also led to reduced eosinophilia and decreased vimentin, transforming growth factor beta (TGF-β) and alpha smooth muscle actin (αSMA) levels. T-$bet^{-/-}$ lung fibroblasts proliferated very rapidly and released increased amounts of TGF-β. Interestingly, neutralization of TGF-β ameliorated aspects of the chronic airway remodeling phenotype but did not reduce AHR. These data highlight a T-bet-directed function for IL-13 in controlling lung remodeling that is both dependent on and independent of its interaction with TGF-β in the asthmatic airway.**

### Introduction

Much experimental evidence indicates a causative relationship between an excessive complement of $T_h2$ cells and the onset of asthma (1). For example, circumstances that prejudice against $T_h1$ development, such as an IL-12 defect, lead to the onset of allergic diseases characterized by over-abundant $T_h2$ cells (2). Mice lacking the $T_h1$-specific transcription factor T-bet have profound defects in the development of the $T_h1$ subset and the production of IFN-γ but over-produce $T_h2$ cytokines (3, 4). Double staining for T-bet and CD4 in lung sections from control subjects revealed that ~50% of CD4+ cells in the airways express T-bet while lungs from patients with asthma displayed decreased numbers of T-bet+ CD4 cells consistent with a shift towards the $T_h2$ phenotype (5). Mice either heterozygous or homozygous for loss of the T-bet gene exhibited airway hyperresponsiveness (AHR) to methacholine associated with a peri-bronchial and peri-vascular infiltration with eosinophils and lymphocytes (5, 6). In contrast to other animal models of asthma, this phenotype occurred spontaneously in the absence of any specific antigenic stimulus or immunological challenge. Interestingly, T-bet heterozygous mice, which have only a 50% reduction of T-bet protein, displayed a phenotype very similar to that of mice with a complete absence of T-bet.

Airway remodeling is a complex feature of chronic asthma and is characterized by increased turnover of the cells and extracellular matrix (ECM) composing the epithelial–mesenchymal unit. One phenotype of chronic remodeling is fibrosis, which is characterized in humans by increased collagen (CL) type III deposition below the basement membrane in the airways. In addition, in chronic asthma there is myofibroblast transformation of mesenchymal cells surrounding the medium- and small-sized bronchi. While transforming growth factor beta (TGF-β) has been described as the major factor involved in *in vitro* fibroblast transformation into myofibroblasts through its effect on the acquisition of intermediate filament proteins such as alpha smooth muscle actin (αSMA), much remains to be learned about the relationship between this cytokine and other potent profibrotic cytokines such as IL-13.

*Received* 18 January 2005, *accepted* 10 May 2005

*Correspondence to*: L. H. Glimcher; E-mail: lglimche@hsph.harvard.edu or S. Finotto; E-mail: finotto@mail.uni-mainz.de

*Transmitting editor*: A. Singer

Advance Access publication 6 July 2005

IL-13-mediated fibrosis depends on the concomitant induction of IGF-1 and suppression of TGF-β. As opposed to TGF-β1, IL-4 and IL-13 can increase fibrosis but cannot alone induce myofibroblast transformation *in vitro* (7–12).

Lungs from T-bet-deficient mice undergo airway remodeling histologically similar to human asthmatic lungs, a process which is accompanied by increased concentrations of both TGF-β1 and IL-13 in bronchoalveolar lavage fluid (BALF) (5, 13). Here we investigate the etiology of this chronic airway remodeling. We demonstrate that in T-bet$^{-/-}$ mice, IL-13 derived from hyperactivated memory CD4 cells controls the asthmatic phenotype observed in T-bet deficiency, in part through its control of TGF-β-driven events.

## Methods

### *Allergen sensitization and challenge and blocking antibody administration*

SV129/C57BL/6/T-bet$^{-/-}$ intercrossed mice (3) (3 months of age) were maintained under specific pathogen-free conditions and received an intra-peritoneal (i.p.) injection of 100 μg ovalbumin peptide (OVA) (Calbiochem, Germany) complexed with alum (Sigma–Aldrich, Taufkirchen, Germany) on days 0 and 7, as previously described (5, 14). On day 7, groups of mice ($n = 6$) received αIL-13 antibody (monoclonal anti-mouse IL-13 antibody; R&D Systems, Germany) (10 or 50 μg as indicated) or αIL-4 (100 μg or 1 mg as indicated) (11B11) by i.p. administration. On day 18, 19 mice were anesthetized with avertine (1 mg tribromethanol per ml *t*-amylalcohol in 2.5% in PBS) before receiving αIL-13 (50 μg per day), αIL-4 (100 μg per day) or αTGF-β1 (50 or 100 μg per day) (R&D Systems) antibodies intra-nasally (i.n.). Control groups ($n = 6$) received either rat IgG 2bκ isotype control antibodies (PharMingen, San Diego, CA, USA) or normal rabbit IgG (R&D Systems). Afterwards, mice were aerosolized with PBS in a chamber connected to an aerosol generator (FMI: Fohr Medical Instruments, Seeheim, Germany). On day 20, airway plethysmography was performed followed by a bronchoalveolar lavage, as described previously (14). Three experiments were performed for αIL-13, αIL-4 and αTGF-β treatment. At least five mice per group were treated and analyzed.

### *Assessment of bronchoconstriction by whole body plethysmograph*

Bronchoconstriction was evaluated by using a non-invasive whole body plethysmograph (model PLY 3211; Buxco Electronics, Inc., Sharon, CT, USA), as previously described (5, 14). Briefly, mice were exposed to 0, 50, 100 mg of methacholine (Sigma) for 3 min by using a sonicator linked to the four exposure chambers, and enhanced pause (Penh) responses of different groups of mice ($n = 6$ mice per group) in the following 5 min were measured. Data are reported as mean value of 30 values of Penh [mean values (Penh) ± SEM] taken every 10 s (5 min) after administration of methacholine.

### *Assessment of AHR and transpulmonary resistance*

To assess AHR, we used a whole body plethysmograph. In this system, an esophageal cannula—water coupled to the pressure transducer—is inserted into anesthetized (pentobarbital), spontaneously breathing mice. The mice are ventilated through a ventilator (Mouse Ventilator, Ugo Basile) with the inlet and outlet of the ventilator connected to the distal end of a previously inserted tracheal cannula. Under these conditions, the transpulmonary pressure (tracheal–esophageal) is monitored. The computed mechanical parameters are the lung resistance (RI) and the lung compliance. In our system, these two parameters are measured with a Resistance/Compliance Isovolumetric analyzer (Buxco Electronics, Inc.) by using a ByoSystem XA software. This analyzer monitors the two inputs flow and pressure from unconscious animals, as well as ventilatory parameters and mechanical parameters on every breath. The resistance parameter is calculated using the common isovolumetric method. In the isovolumetric method, the flow changes are measured by finding the difference between the inspiratory flow and expiratory flow measured at a certain volume. The pressure changes are measured in the same way. Airflow is calibrated by using the Int-Zero calibration method (also used for the Penh measurements) with 1-ml air injection. The pressure is calibrated using a water manometer attached to the transducer in accordance with the two-point reading method. Both calibrations were performed according to the manufacturer's instructions (Buxco, Electronics, Inc., BioSystem XA for window). At the beginning of the experiment, different doses of methacholine were instilled intra-tracheally by placing 10 μl of the chosen methacholine concentrations in the in-line aerosol system connected to the plethysmograph.

### *Isolation and analysis of lung CD4+ T cells*

Lung pieces were placed in DMEM (GIBCO) and incubated at 37°C for 1 h in Dulbecco's PBS containing 300 U ml$^{-1}$ of collagenase type II (Worthington Biochemical Corporation, Lakewood, NJ, USA) and 0.001% DNase (Roche Diagnostics, Heidelberg, Germany). The suspension was then filtered through a 70-μm nucleopore filter (Nunc). After centrifugation, the cell pellet was washed in MACS buffer (PBS/EDTA with 3% FCS; BioWhittaker Europe, Cambrex Company, Verviers, Belgium) followed by incubation with anti-mouse CD4 antibodies bound to beads ($10^7$ Dynabeads CD4-L3T4 ml$^{-1}$; 25 μl beads for $2.5 \times 10^6$ cells) for 20 min at 4°C under shaking conditions. Lung CD4+ cells were isolated by positive magnetic selection in accordance with the manufacturer's instructions. αCD4 beads were detached by using mouse CD4 DETACHaBEAD (Dynal, Hamburg, Germany). CD4+ cells were cultured with soluble αCD28 and plate-bound αCD3 antibodies (CD3, clone 145-2C11, 5 μg ml$^{-1}$; CD28, clone 37.51, 2 μg ml$^{-1}$; PharMingen) overnight at a density of $10^6$ cells ml$^{-1}$. Supernatants were analyzed for cytokine production by ELISA as described below. The cell pellet was processed for RNA extraction.

To analyze lung CD4 T cell activation, naive, untreated T-bet-deficient and wild-type (wt) mice on a SV129/B6 genetic background were analyzed. CD4+ T cells were directly purified from isolated lung cell suspensions using αCD4+ mouse bead-conjugated mAbs (Miltenyi, Bergisch Gladbach, Germany) in a multiparameter magnetic sorter system (MACS, Miltenyi). The resulting CD4+ cells (purity 97%) were further

stained with an anti-mouse CD4–PE-conjugated antibody (PharMingen), with αCD69–FITC-conjugated and anti-mouse CD44–CyChrome-conjugated antibodies for 30 min at 4°C, washed twice in PBS and then analyzed by FACS analysis with a FACSCalibur (BD PharMingen).

*Isolation and functional analysis of lung CD4+CD25+ cells*

Isolation of CD4+CD25+ T regulatory cells (Treg) was performed after bead detachment of isolated CD4+ T lung cells derived either from untreated wt or T-bet$^{-/-}$ mice (Fig. 1A) on a SV129/B6 genetic background. In additional experiments (Fig. 6A), CD4+CD25+Tregs were isolated from T-bet$^{-/-}$ mice that had been sensitized i.p. with OVA as described above and challenged with PBS and *in vivo* treated either with normal rabbit serum or αTGF-β antibodies i.n. The method of isolation of lung CD4+CD25+ cells is described below.

After bead detachment, enriched CD4+ lung cells derived from either untreated wt or T-bet$^{-/-}$ SV129/B6 mice were stained with CD25–PE antibody followed by incubation with anti-PE beads and immunomagnetic separation (CD25 Microbead Kit mouse, Miltenyi Biotech). Lung CD4+CD25+ ($10^5$ cells per well) cells or CD4+CD25− ($10^5$ cells per well) were then co-cultured with CFSE-labeled (Molecular Probes, Leiden, The Netherlands) target primary CD4+CD25− lung cells ($10^5$ cells per well), isolated from the same untreated mice, along with mitomycin C-treated (60 μg/ml/$10^7$ cells for 30 min) antigen presenting cells (A20, a murine B lymphoma cell line; $10^4$ cells per well) and in the presence of soluble αCD3 antibodies (2.5 μg ml$^{-1}$) overnight. After 20 h, the starting incorporated fluorescence was recorded (M1). The proliferation of the target lung CD4+CD25− (CFSE+) cells was then taken from the percentage of daughter cells that would reach generation (or mitosis = M) M5 or M6. Two to three pools with two lungs per pool were analyzed for each experimental group. In separated cell cultures, sorted lung CD4+CD25+ ($10^5$ cells per well) cells or CD4+CD25− ($10^5$ cells per well) cells were cultured with 2 μg ml$^{-1}$ αCD3 (PharMingen). Supernatants were then collected and IL-10, IL-5, IL-4 measured by ELISA (Fig. 6B). Purity of CD4+CD25+ T cell populations was assessed by measuring Foxp3 transcripts.

*Lung fibroblast cell culture*

Lung fibroblasts were grown from lung cell suspensions from untreated mice (3 months of age) immediately after enzymatic digestion or from the CD4−− fraction after CD4++ cell isolation as described above. Lung cells were then seeded at a density of $10^6$ cells ml$^{-1}$ in 24-well plates and cultured in DMEM with high glucose, glutamine, pyruvate, 1% penicillin/ptreptomycin and amphotericin B (250 mg L$^{-1}$) (Biochrom AG, Berlin, Germany) and 10% FCS overnight. The day after, supernatants with dead cells were removed and the adherent cells further cultured to semi-confluence. Semi-confluence typically occurred after 5 days when fibroblasts were isolated from T-bet$^{-/-}$ lung and after 2 weeks from wt lung. On day 5, cells were washed in PBS and then cultured in DMEM medium minus amphotericin B and the serum concentration was reduced to 0.4% overnight. Supernatants were collected the day after (day 6) and analyzed for TGF-β production by ELISA (Fig. 7H) and fibroblast cultures frozen for subsequent immunocytochemical studies.

*Immunohistochemistry*

Fibroblasts and myofibroblasts were immunostained directly in culture wells as previously described with some modifications (18). Briefly, fibroblasts were fixed in 2% PFA, permeabilized with permeabilization buffer (0.3% Triton X-100 in PBS) and washed twice in Tris-buffered saline (TBS) buffer (0.05 M Tris–hydrochloride). After 1 h incubation in blocking buffer (3% BSA, 0.05% Tween 20 in TBS), the rabbit polyclonal anti-vimentin antibody (Santa Cruz Biotechnology, Heidelberg, Germany) was applied (1: 100) in antibody diluent (Dako, Carpinteria, CA, USA) and incubated overnight at 4°C. The following day a goat anti-rabbit biotinylated antibody (Vector Laboratories, Burlingame, OA, USA; 1: 200 in blocking buffer) was applied followed by incubation with Cy3–streptavidin. Detection of αSMA+ cells was performed after further incubation with monoclonal αSMA (1: 100; Sigma) followed by incubation with a biotinylated horse anti-mouse antibody followed by Cy3–streptavidin (1: 500 in PBS). SMAD3 and SMAD7 proteins were detected by immunofluorescence using anti-SMAD3 and anti-SMAD7 rabbit polyclonal antibodies (Santa Cruz Biotechnology) followed by incubation with a biotinylated goat anti-rabbit antibody (Vector Laboratories; 1: 200 in blocking buffer) followed by Cy2–streptavidin green fluorochrome (1: 500 in PBS) (Fig. 6C).

*ELISA*

Mouse IL-4, IL-5, IFN-γ and IL-10 were detected using a specific sandwich ELISA (OptEIA™, BD PharMingen). Murine IL-13 was detected using an ELISA kit (R&D Systems). TGF-β analysis was performed by using purified rat anti-mouse, human, pig TGF-β1 as capture antibody (PharMingen, Heidelberg, Germany) and biotinylated rat anti-mouse, human, pig TGF-β1 (PharMingen) polyclonal antibody. Recombinant TGF-β was purchased from R&D Systems. To activate latent TGF-β, 200-μl samples was pre-treated with 10 μl of 1 N HCl for 30 min at 37°C. Samples were then neutralized by adding 10 μl of 1 N NaOH.

*Protein extraction, western blot analysis and immunoprecipitation*

Tissue proteins were extracted as previously described from naive untreated mice (14). Briefly, tissue was homogenized in PBS and protein extracted in the presence of protease inhibitors. After boiling for 2 min, proteins were separated by 10 or 15% SDS-PAGE, transferred to nitrocellulose membranes washed briefly in PBS and incubated in blocking solution (5% milk in PBS/0.05% Tween 20) for 1 h at room temperature, and subsequently exposed to 1 μg ml$^{-1}$ of antibodies against β-actin, SMAD3 (Santa Cruz Biotechnology) or αSMA and anti-vimentin (Sigma), in blocking solution. Specific binding was visualized with the ECL western blotting detection system according to the manufacturer's instruction after 1 h incubation with the corresponding secondary HPR-conjugated antibody (1: 2000 in blocking solution) (Amersham Pharmacia Biotech, Germany).

For immunoprecipitation, 250 μg total lung proteins was precleared with 1 μg of appropriate IgG according to the primary antibody and 20 μl A/G plus agarose (Santa Cruz Biotechnology) for 30 min at 4°C. After centrifugation at 2500 r.p.m.

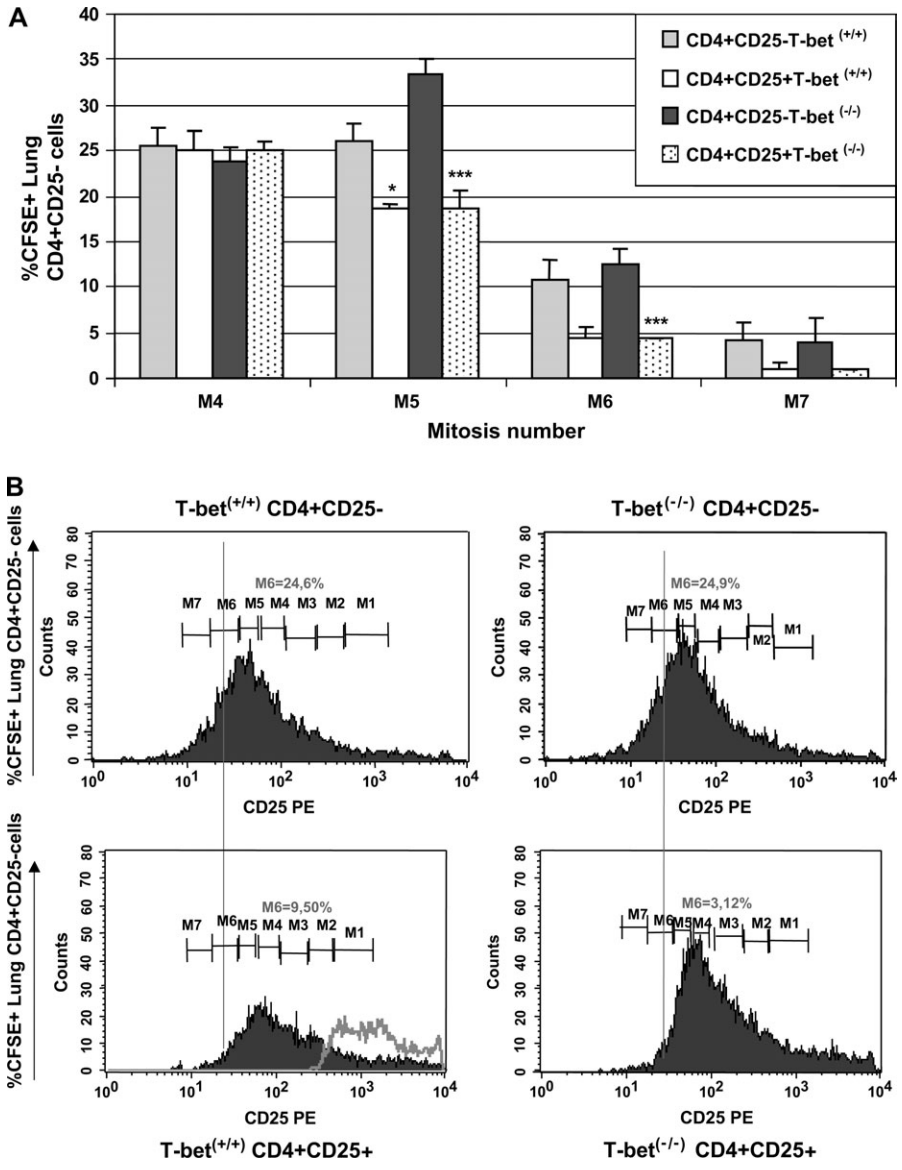


**Fig. 1.** T-bet$^{-/-}$ lung CD4+CD25+ Tregs have normal immunosuppressive function but T-bet$^{-/-}$ lung CD4+CD25− cells have a predominantly activated/ memory phenotype. (A) CD4+CD25+ cells isolated from the lung of T-bet$^{-/-}$ mice suppress the proliferation of CD4+CD25− lung cells isolated from the same mouse. Different cell generations are shown (M1 to M7) ($n = 4$ per group). (B) Representative histograms of CD4+CD25− CFSE-labeled cells 4 days after the beginning of cell culture (M1). A vertical lane was drawn at M6 which indicates the percentage of naive lung CD4+CD25− cells (wt on the left and T-bet$^{-/-}$ on the right) reaching the sixth generation after 4 days of cell culture either in the presence of CD4+CD25− (upper panels) or CD4+CD25+ cells (lower panels). (C) CD4+ T cells were isolated from wt and T-bet$^{-/-}$ lung as described in Methods and then immunostained with αCD4–cytochrome-, αCD69–FITC-, αCD44–PE-conjugated antibodies and analyzed by FACS. Results represent three mice per group. (D) The upper and lower left panels show quantification of activated/memory (CD69$^{high}$CD44$^{high}$) cells in the isolated lung CD4+CD25− cell fraction. T-bet$^{-/-}$ mice have increased percentages (upper panel) and absolute numbers (lower panel) of lung CD44$^{high}$CD69$^{high}$ cells as compared with wt mice within the lung CD4+CD25− cell population. The absolute number of lung CD4+CD25+ cells are shown (right panel). Lower right panel: Foxp3 and actin expression in lung CD4+CD25− and CD4+CD25+ cells measured by reverse transcription–PCR. Isolated wt lung CD4+CD25+ cells express Foxp3 while CD4+CD25− cells do not.

for 5 min, supernatant was collected and incubated with 2 μg primary antibody (SMAD3) for 1 h at 4°C followed by addition of 20 μl of A/G plus agarose. The immunoprecipitation was completed by incubation at 4°C overnight under rotating conditions. The next day, the pellet was washed four times with PBS and re-suspended in 50 μl PBS. Western blots were performed as described above with one-third of immunoprecipitated protein, blotted in a nitrocellulose membrane and incubated with anti-phosphoserine residues of SMAD2 and 3 (Upstate, Milton Keynes, UK).

### *Statistical analysis*

Differences were evaluated for significance ($P < 0.05$) by the Student's two-tailed *t*-test for independent events (Excel, PC). Data are given as mean values ± SEM.

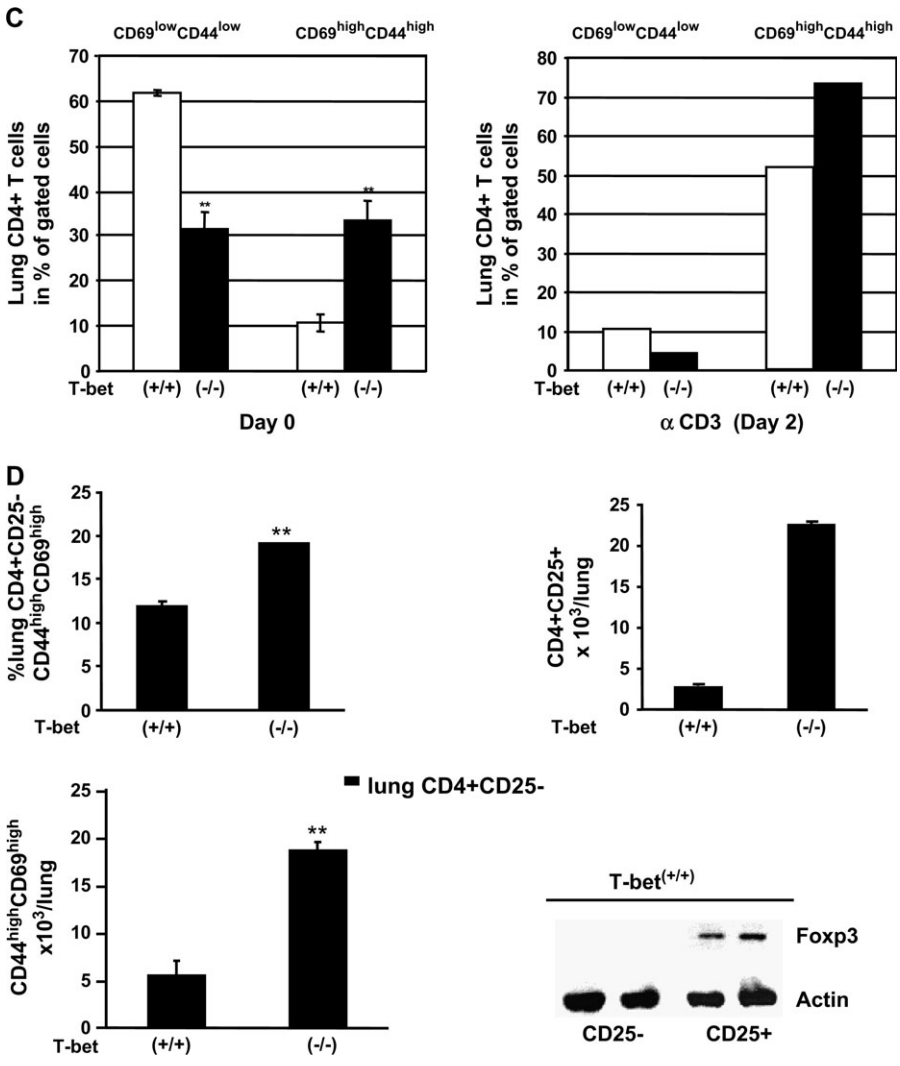


**Fig. 1.** *Continued.*

## Results

*Isolation of functionally intact lung CD4+CD25+ Tregs but increased numbers of activated/memory CD4+ T cells from T-bet$^{-/-}$ mice*

We previously reported that T-bet$^{-/-}$ mice, without allergen challenge, develop hallmark features of asthma with airway inflammation and hyperresponsiveness. Further, immunodeficient mice reconstituted with OVA-specific T-bet$^{-/-}$ spleen CD4+ cells developed airway inflammation and hyperresponsiveness, demonstrating a direct relationship between CD4+ T cells and the asthma phenotype (5). Recent reports have suggested a role for CD25+CD4+ regulatory T cells in inhibiting asthma. Patients with mutations in the transcription factor Foxp3 and hence deficiencies in CD4+CD25+ Tregs (IPEX) present with severe eczema, elevated IgE, eosinophilia and food allergy (19). However, we have previously reported the presence of an increased rather than a decreased number of Tregs in the absence of T-bet in an adoptive transfer model of inflammatory bowel disease (20). Nevertheless, we asked whether T-bet$^{-/-}$ mice develop asthma due to a defect in Treg function. CD4+CD25+ and CD4+CD25− cells were isolated directly from the lungs of wt and T-bet$^{-/-}$ untreated mice. Lung CD4+CD25− cells were then labeled with CFSE and co-incubated either with CD4+CD25+ or CD4+CD25− lung T cells in a 1: 1 ratio. Figure 1(A and B) shows that T-bet$^{-/-}$ CD4+CD25+ cells inhibited CD4+CD25− cell proliferation as effectively as did wt CD4+CD25+ T cells, indicating that T-bet$^{-/-}$ mice develop functionally intact immunosuppressive CD4+CD25+ cells in the lung. We conclude that the asthmatic phenotype we observe cannot be accounted for by an impairment in CD4+CD25+ Tregs in the absence of T-bet. In addition, very recent data suggest that freshly isolated CD4+CD25+ cells are not able to suppress $T_h2$ cells but require pre-activation with co-stimulatory signals *in vitro* to suppress proliferation and induce Foxp3 in $T_h2$ cells (21).

We therefore tested whether conventional lung CD4+ cells might be spontaneously activated in the absence of T-bet. Indeed, lung CD4+ T cells isolated from T-bet$^{-/-}$ untreated mice contained a higher percentage of cells with an

activated/memory phenotype as compared with littermate controls. As shown in Fig. 1(C, left panel), there were approximately equal numbers (30%) of naive (CD44$^{low}$CD69$^{low}$) and memory (CD44$^{high}$CD69$^{high}$) CD4+ T cells present in T-bet$^{-/-}$ lung. In contrast, the majority (up to 60%) of CD4+ cells isolated from wt littermates was of the naive phenotype with only a small number (10%) of memory-type T cells. Forty-eight hours after αCD3 stimulation, the number of T-bet$^{-/-}$ memory cells further increased (up to 80 versus 60% in wt) (Fig. 1C, right panel) and co-stimulatory activation through αCD28 antibodies had no influence on these activation parameters (data not shown). Furthermore, both the percentage and number of activated/memory cells were increased in the T-bet$^{-/-}$ lung CD4+CD25− cell compartment as compared with wt. The efficiency of isolation and separation of the two populations was confirmed by the presence of Foxp3 transcripts in the CD4+CD25+ but not CD4+CD25− populations (Fig. 1D). We conclude that in the absence of T-bet the ratio of activated/memory to naive lung CD4 T cells is greatly increased relative to what is observed in wt mice.

### *Lung CD4+ T cells from T-bet$^{-/-}$ mice release increased $T_h$2 cytokines*

T-bet controls $T_h$1 differentiation in part through direct transcriptional activation of the IFN-γ gene and up-regulation of IL-12Rβ2 chain expression (22–27). An equally important function of T-bet resides in its ability to repress $T_h$2 cytokine gene expression by a mechanism independent of IFN-γR signaling (22). We previously reported that T-bet$^{-/-}$ mice spontaneously release increased amounts of $T_h$2 cytokines in the periphery and in the airways as measured in BALF (5). We wished to establish the cytokine profile of CD4+ T cells isolated directly from the lung. As shown by ELISA in Fig. 2, T-bet$^{-/-}$ lung CD4+ T cells, isolated from untreated mice, produced IL-4 (A), IL-5 (B) and IL-13 (C) after stimulation with αCD3 alone in contrast to wt littermates. This was presumably secondary to the activated versus naive status of T-bet$^{-/-}$ compared with wt lung CD4 T cells. Upon co-stimulation with αCD28, the amount of IL-4 and IL-5 produced by T-bet$^{-/-}$ T cells was further increased (Fig. 2A). Of particular interest was the over-production of IL-13 by T-bet$^{-/-}$ as compared with wt lung CD4 cells. Indeed, after OVA sensitization, levels of IL-13 (D) increased further, reaching ~6 ng ml$^{-1}$, a very high value.

### *Local blockade of IL-4 and IL-13 ameliorates airway inflammation in T-bet$^{-/-}$ mice*

A hallmark feature of asthma is airway inflammation, characterized by peri-vascular and peri-bronchial infiltration of the airways with eosinophils and lymphocytes. We previously reported that T-bet$^{-/-}$ mice, in the absence of any immunological challenge, had increased infiltration of eosinophils and lymphocytes in airways as assessed by histologic analysis. To more precisely quantitate the cellular infiltrate, we examined BALF of untreated wt and T-bet$^{-/-}$ mice. T-bet$^{-/-}$ mice had increased overall cell numbers in BALF (total cell number × $10^3$ ml$^{-1}$ of BALF: T-bet$^{+/+}$ 19.16 ± 8.8 and T-bet$^{-/-}$ 486.66 ± 200.3, $P$ = 0.026), including eosinophils (total eosinophils number × $10^3$ ml$^{-1}$ of BALF: T-bet$^{+/+}$ 0.33 ± 0.15 and

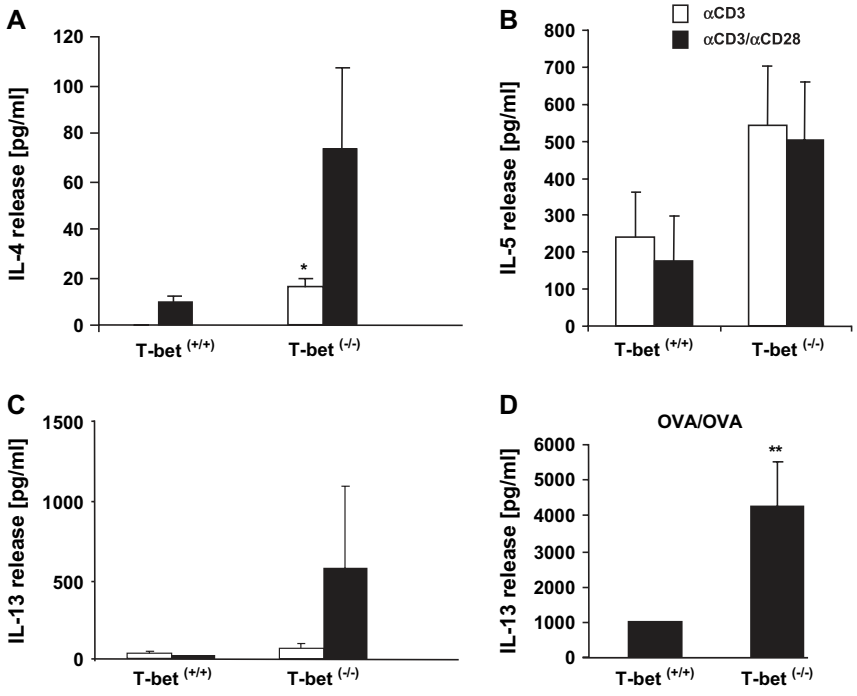


**Fig. 2.** Lung CD4 cells isolated from T-bet-deficient mice release increased amounts of IL-4, IL-5 and IL-13. Lung CD4 cells isolated from untreated wt and T-bet$^{-/-}$ mice were stimulated overnight with αCD3 alone or with αCD3/CD28 and cytokines released in the supernatant measured by ELISA. In (D), IL-13 was measured in the supernatant of lung CD4+ cells isolated from OVA-sensitized and OVA-challenged mice.

T-bet$^{-/-}$ 458.01 ± 209.1, $P = 0.049$), confirming the previous histological analysis. Both IL-4 and IL-13 contribute to the asthmatic phenotype. To ask whether these cytokines, whose levels were increased in T-bet$^{-/-}$ lung, were involved in the asthmatic phenotype, we neutralized IL-13 and IL-4 by i.p. and i.n. delivery of specific antibodies. As shown in Fig. 3A, i.n. blockade of either IL-13 (50 μg i.p. on day 7 and 50 μg per day for 2 days i.n. on days 18 and 19) or IL-4 (1 mg i.p. on day 7 and 100 μg per day i.n. on days 18 and 19), in OVA-sensitized mice, suppressed the number of eosinophils in the BALF as compared with control IgG (100 μg i.p. and 100 μg per day on days 18 and 19). IL-5 is the major growth and differentiating factor for eosinophils. Consistent with the reduction in eosinophil number, αIL-13 treatment led to decreased IL-5 production in the BALF of treated mice (Fig. 3B). We also examined whether IL-13 blockade affected the production of cytokines specifically from CD4 T cells. Indeed, treatment with IL-13 antibody reduced IL-5 production from CD4 T cells (Fig. 3C). Interestingly, levels of the protective cytokine IFN-γ, although low as expected in the absence of T-bet, were increased after treatment with IL-13 antibody, suggesting that non-T-bet-dependent IFN-γ production was IL-13 mediated (Fig. 3D).

### *Local blockade of IL-13 but not IL-4 or TGF-β ameliorates bronchoconstriction in T-bet$^{-/-}$ mice*

We next asked therefore whether local blockade of IL-4 or IL-13 would ameliorate the spontaneous AHR observed in T-bet$^{-/-}$ mice. In an initial series of experiments, we found that i.n. blockade of IL-4 in OVA-sensitized mice did not lead to a decrease in bronchoconstriction, even when antibodies were given for 2 days i.n. (100 μg per day). Since levels of IL-4 are elevated in T-bet$^{-/-}$ mice in the periphery as well as the lung, we also blocked IL-4 systemically by injecting 1 mg of αIL-4 antibody i.p. during the second OVA sensitization on day 7 before giving αIL-4 i.n. on days 18 and 19 (100 μg per day); however, no effect on bronchoconstriction after methacholine challenge, as compared with IgG control treatment, was observed (Fig. 4A). Similarly, local blockade of TGF-β i.n. for 2 days on days 18 and 19 (100 μg per day) did not reduce bronchoconstriction in T-bet$^{-/-}$ mice (Fig. 4C), nor did blockade of TGF-β reduce the release of IL-13 (Fig. 4D). In contrast, OVA-sensitized T-bet$^{-/-}$ mice that received αIL-13 antibodies i.n. (50 μg per day at days 18 and 19) prior to delivery of aerosol PBS displayed significantly decreased bronchoconstriction as shown in Fig. 4B, where AHR was measured 24 h after the last antibody dose in response to different doses of methacholine. These results demonstrate a direct effect of IL-13 but not IL-4 or TGF-β on the elevated airway bronchoconstriction in T-bet$^{-/-}$ mice.

### *Local blockade of IL-13 but not IL-4 ameliorates AHR in T-bet$^{-/-}$ mice*

We also measured lung resistance (RI) in OVA-sensitized wt and T-bet$^{-/-}$ mice treated i.n. with either αIL-13 or αIL-4 antibodies prior to PBS challenge (OVA/PBS). As shown in Fig. 4F, αIL-13 but not αIL-4 antibody treatment had a protective effect on the development of AHR in

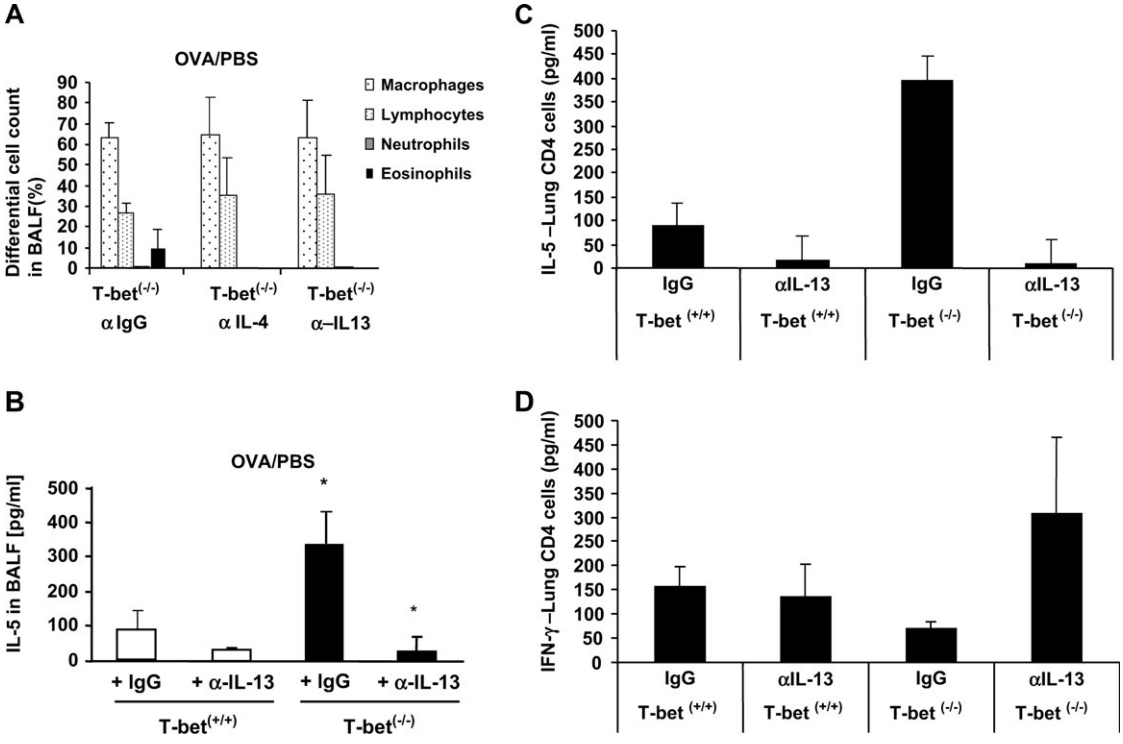


**Fig. 3.** Effect of local αIL-13 and αIL-4 antibody treatment in T-bet$^{-/-}$ lung. (A) Local application of αIL-13 (50 μg i.p. on day 7 and 50 μg i.n. per 2 days at the time of PBS challenge) and αIL-4 antibody (100 μg i.p. and 100 μg i.n. at the time points indicated) reduces eosinophil counts in T-bet$^{-/-}$ BALF as compared with IgG control antibody. (B) αIL-13 treatment reduces levels of IL-5 in BALF of T-bet$^{-/-}$ mice. αIL-13 treatment down-regulates IL-5 (C) and up-regulates IFN-γ (D) production in lung CD4+ T cells isolated from T-bet$^{-/-}$ mice.

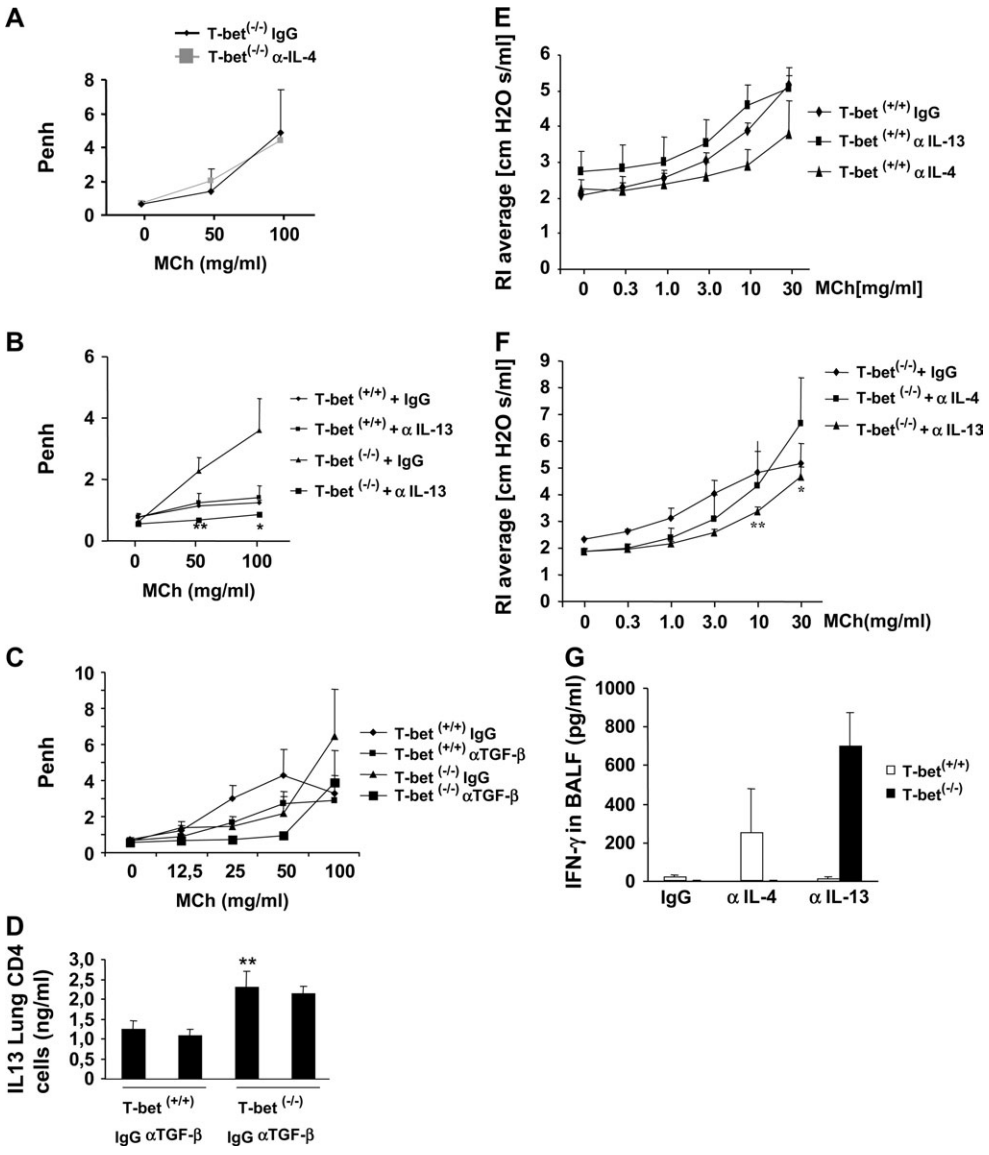


**Fig. 4.** αIL-13 but not αIL-4 or αTGF-β antibody treatment ameliorates AHR in T-bet$^{-/-}$ mice. (A) IL-4 blockade did not ameliorate bronchoconstriction after i.p. injection of 1 mg ml$^{-1}$ of αIL-4 antibodies during the OVA-sensitization phase and i.n. on days 18 and 19 (100 μg ml$^{-1}$ per day) 30 min before PBS challenge (OVA/PBS). Results are expressed as average Penh values collected during the first 5 min. Dose response after 3-min delivery of increasing doses of methacholine (MCh) (0, 50, 100 mg ml$^{-1}$) are reported ($n = 6$). Three experiments per treatment group were performed. (B) Intra-nasal delivery of αIL-13 antibodies results in significant amelioration of AHR in T-bet$^{-/-}$mice as compared with IgG2B-treated mice after exposure to 100 mg ml$^{-1}$ of MCh. Results are reported as mean of Penh ± SEM of $n = 6$ mice per group. Three experiments for each group were performed. Shown is one representative experiment out of three. Average Penh is obtained from 30 values taken every 10 s for the first 5 min after MCh delivery. (C and D) TGF-β blockade did not ameliorate bronchoconstriction (C) or decrease IL-13 production (D) after i.n. injection for 2 days on days 18 and 19 (100 μg per day). Five to six SV129/C57BL/6 wt or T-bet (−/−) mice per group were sensitized to OVA followed by local treatment with PBS aerosol (OVA/PBS) after i.n. treatment with αIL-4 (50 μg per day), αTGF-β (100 μg per day) or αIL-13 (50 μg per day) antibodies. Body plethysmography was performed 24 h after the last local treatment in all mice, as specified in Methods. Dose–response curves to MCh were obtained after administrating indicated doses of aerosolized MCh. αIL-13-treated, T-bet$^{-/-}$/OVA-sensitized mice were protected from AHR as compared with αIL-4-, αTGF-β- or IgG-treated, OVA-sensitized mice. No significant changes were observed after antibody treatment of wt littermates (B and C). (E and F) Airways resistance (RI) in OVA-sensitized wt and T-bet$^{-/-}$ mice treated i.n. with either αIL-13 or αIL-4 antibodies prior to PBS challenge (OVA/PBS). (G) αIL-13 but not αIL-4 treatment also led to an increase in IFN-γ in the BALF of T-bet$^{-/-}$ mice while in wt mice, αIL-4 antibody treatment slightly increased IFN-γ.

T-bet$^{-/-}$ mice. The effect of αIL-4 and αIL-13 antibody treatment on AHR of OVA/PBS-treated wt mice is shown for comparison in Fig. 4(E). These differences may be explained by our finding that αIL-4, but not αIL-13, treatment led to up-regulation of IFN-γ in wt airways while just the reverse was true for T-bet$^{-/-}$ mice where IFN-γ was increased by αIL-13 but not by αIL-4 treatment (Fig. 4G). Taken together, these data indicate a T-bet independent, protective effect likely mediated by IFN-γ in the lung of αIL-13-treated mutant mice.

*Activation of TGF-β signal transduction in T-bet$^{-/-}$ mice*

Airway remodeling is a complex feature of chronic asthma and is characterized by increased cell turnover and ECM formation composing the epithelial–mesenchymal unit. One phenotype of chronic remodeling is fibrosis, which is characterized in humans by increased CL type III deposition below the basement membrane in the airways. In addition, in chronic asthma there is myofibroblast transformation in mesenchymal cells surrounding the medium- and small-sized bronchi. TGF-β has been described as the major factor involved in *in vitro* fibroblast transformation into myofibroblasts through acquisition of intermediate filament proteins such as αSMA (13, 28–32).

Along with increased CL deposition, we have previously found increased transformation of fibroblasts into myofibroblasts in T-bet$^{-/-}$ lungs and increased levels of TGF-β in the BALF of T-bet$^{-/-}$ mice (5). To examine the activation of TGF-β signal transduction in the presence or absence of T-bet in the lung, we immunoprecipitated total lung proteins from untreated wt and T-bet$^{-/-}$ mice with αSMAD3S antibody and immunoblotted them with an antibody directed against the phosphoserine residues of SMAD3S–SMAD2. As shown in Fig. 5(A), increased phosphorylated SMAD3–SMAD2 complexes were present in proteins immunoprecipitated from the lung of T-bet$^{-/-}$ mice as compared with wt mice, indicating increased activation of TGF-β signal transduction in the former.

*αIL-13 treatment inhibits TGF-β production in T-bet$^{-/-}$ lungs*

αIL-13 as well as αIL-4 blockade decreased TGF-β production in the BALF as compared with control IgG treatment, although αIL-13 was slightly more potent (Fig. 5B). However, TGF-β is produced by many cells in the lung, including CD4+ T cells. We therefore analyzed TGF-β release in lung CD4+ T cells isolated from αIL-13- or αIL-4-treated T-bet$^{-/-}$ mice that had been incubated overnight with αCD3 antibody. As shown in Fig. 5(C), IL-13 ($P = 0.0057$) but not IL-4 blockade reduced levels of TGF-β from T-bet$^{-/-}$ CD4+ T cells. We conclude that while both IL-13 and IL-4 control TGF-β production in BALF, only IL-13 can control its production in CD4 T cells, at least in the absence of T-bet.

*TGF-β blockade does not alter the function of T-bet$^{-/-}$ CD4+CD25+ lung Tregs or production of $T_h$2 cytokines from effector T-bet$^{-/-}$ CD4+CD25– cells*

TGF-β over-production might have consequences for immune system cells as well as for epithelial and mesenchymal cells in the T-bet$^{-/-}$ lung. We analyzed its effect on lung CD4+CD25+ Tregs isolated from T-bet$^{-/-}$ mice treated i.n. with αTGF-β or IgG control antibodies. As shown in Fig. 6A, αTGF-β local treatment *in vivo* did not change the suppressive function of T-bet$^{-/-}$ CD4+CD25+ Tregs. T-bet$^{-/-}$ lung CD4+CD25+ cells harvested from OVA/PBS/αTGF-β-treated mice inhibited the CFSE-labeled effector cell population as effectively as did lung CD4+CD25+ cells isolated from T-bet$^{-/-}$ αIgG-treated mice (Fig. 6A). In addition, local blockade of TGF-β in the lung did not change $T_h$2 cytokine production in lung $T_h$2 effector cells (Fig. 6B). The wt lung CD4+CD25+ cell population was Foxp3 positive as found by reverse transcription –PCR, and TGF-β blockade led to down-regulation of Foxp3 expression (Fig. 6B). Taken together, these data indicate that blockade of IL-13, and hence blockade of TGF-β must ameliorate asthma via mechanisms that involve cells other than or in addition to

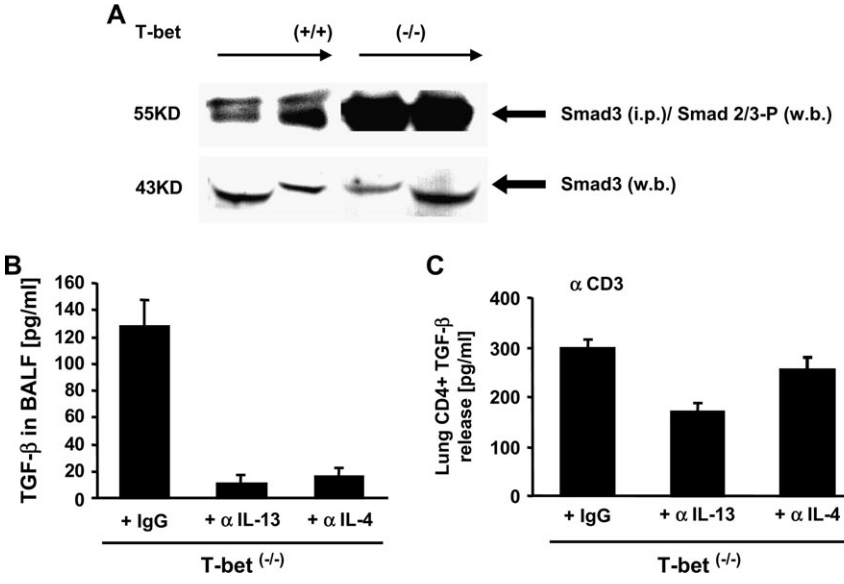


**Fig. 5.** Increased TGF-β signaling in T-bet$^{-/-}$ lung is inhibited by αIL-13 antibody treatment. (A) T-bet$^{-/-}$ lung has increased SMAD3SMAD3-2 phosphorylation. Total lung proteins were isolated, immunoprecipitated with αSMAD3 antibody and probed with an antibody directed against phosphoserine residues of both SMAD2 and 3. In the lower panel, a direct SMAD3 western blot is shown as loading control. (B) αIL-13 (i.n.) and αIL-4 (i.n.) antibody treatment leads to down-regulation of TGF-β in the airways of treated mice ($n = 6$) as shown by ELISA analysis of BALF samples. (C) CD4+ T cells isolated from the airways of T-bet$^{-/-}$ mice release TGF-β, which is down-regulated by αIL-13 but not αIL-4 treatment ($n = 6$).

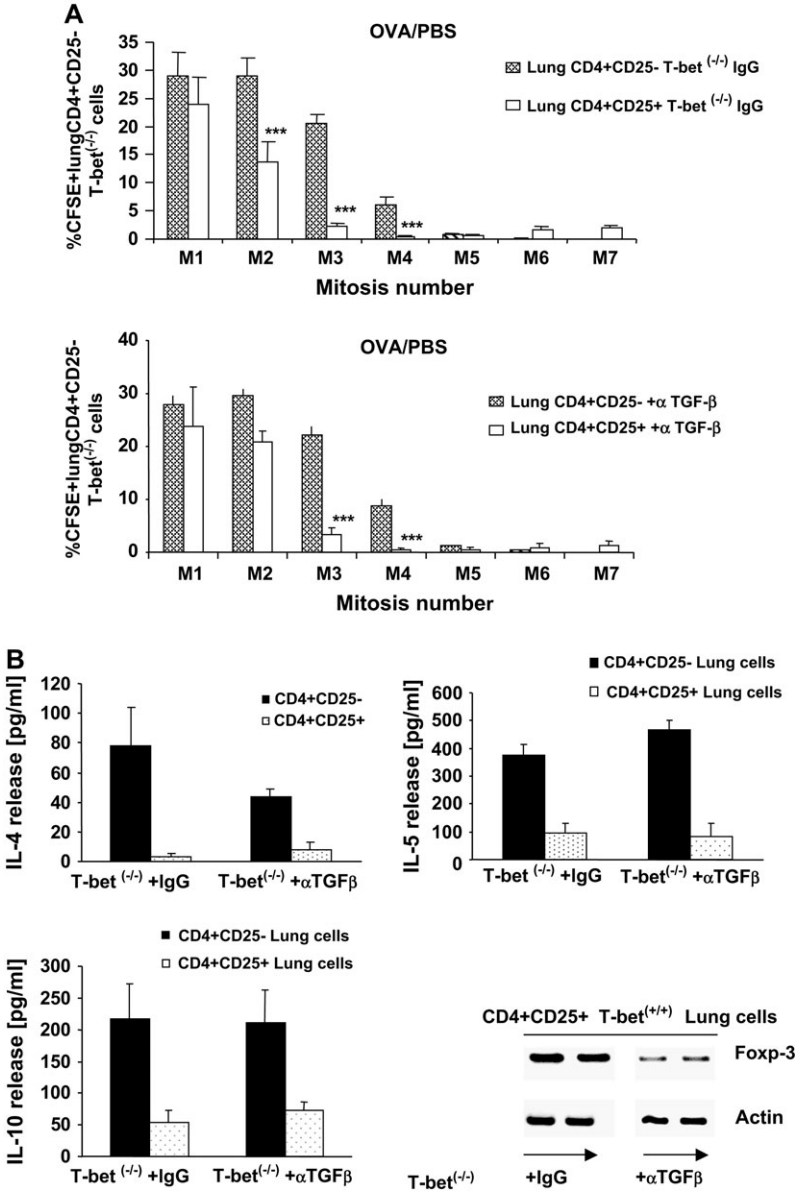


**Fig. 6.** Down-regulation of TGF-β by αTGF-β antibody treatment does not change lung CD4+CD25+ Treg and CD4+CD25− T effector cell properties. OVA-sensitized and PBS-challenged (OVA/PBS) T-bet$^{-/-}$ mice were treated twice with αTGF-β antibodies or IgG control antibodies i.n. (50 μg per day) during the challenge phase. Either lung CD4+CD25+ Tregs or unlabeled CD4+CD25− cells were isolated and co-cultured with CFSE-labeled CD4+CD25− lung cells isolated from the same mouse. (A) T-bet$^{-/-}$ Tregs are as suppressive as wt Tregs. Inhibition of lung CD4+CD25− effector cell proliferation was analyzed by FACS 4 days after the beginning of the cell culture after *in vivo* treatment with IgG (upper panel) or αTGF-β (lower panel). Results are expressed as percentage of gated proliferating cells at a given generation (M = mitosis). (B) No difference in relative amounts of $T_h2$ cytokines upon TGF-β treatment. IL-4, IL-5 and IL-13 cytokines from each population were measured by ELISA. Foxp3 expression as measured by reverse transcription–PCR is decreased after TGF-β treatment of wt CD4+CD25+ cells.

Tregs. Further, TGF-β does not itself alter cytokines produced by CD4+ cells.

### *αSMA and vimentin expression is reduced by αIL-13 but not by αIL-4 treatment*

To understand the mechanism by which IL-13 blockade decreases the asthmatic phenotype of T-bet$^{-/-}$ mice, we analyzed the expression of proteins that characterize chronic airway remodeling in chronic asthma. As shown in Fig. 7A, blockade of IL-13 but not IL-4 led to reduced expression of vimentin, an intermediate intra-cytoplasmic filament expressed in fibroblasts. In addition, IL-13 blockade led to decreased expression of αSMA, the signature protein of myofibroblasts. A direct role of IL-4 on fibrosis has not previously been clearly demonstrated (33–35). We conclude that, at least in the setting of T-bet deficiency, IL-13, but not IL-4, controls both fibrosis and remodeling as assessed by vimentin and αSMA expression, respectively (Fig. 7A). IL-4

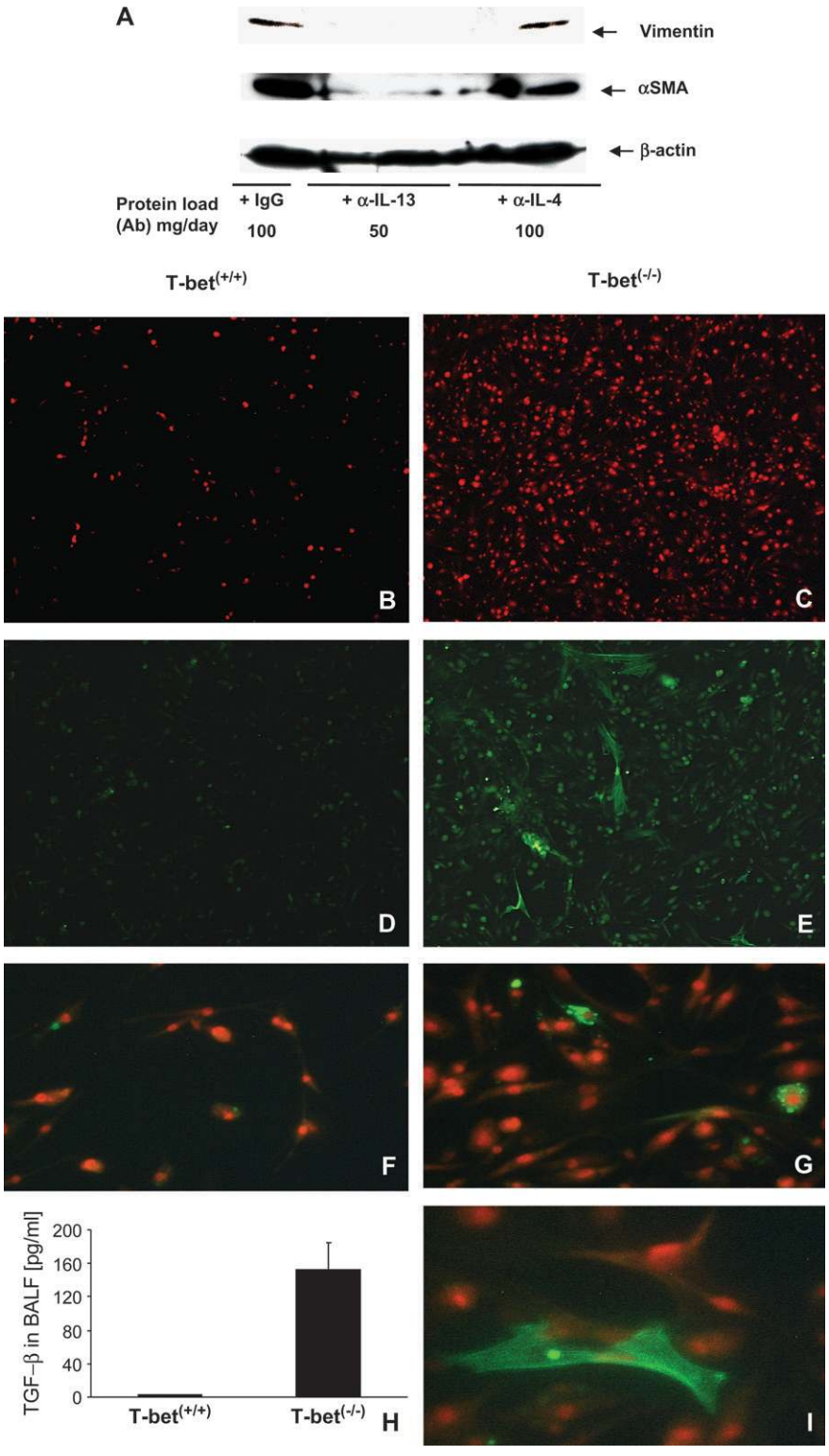


**Fig. 7.** (A) Increased remodeling in the mesenchymal compartment of the T-bet$^{-/-}$ lung is mediated by IL-13. Western blot analysis of total lung proteins after immunostaining for vimentin (a marker for fibroblasts) and αSMA (a marker for myofibroblasts) is shown. The expression of both proteins was down-regulated in the lung of αIL-13 (two mice out of five analyzed are shown) but not αIL-4 treatment of OVA/PBS-treated mice (two mice out of five are shown) as compared with IgG-treated mice. β-Actin is shown as loading control. (B–H) Increased proliferation and TGF-β production by lung fibroblasts isolated from T-bet$^{-/-}$ mice. Fibroblasts isolated from the lung of untreated T-bet$^{-/-}$ mice (right panel: C, E and G and I) proliferate faster and undergo more pronounced myofibroblast transformation compared with wt (left panel: B, D and F). Green is αSMA and red is vimentin. Pictures were taken at ×200 magnification with a Zeiss inverted fluorescence microscope. (H) TGF-β production *ex-vivo* from fibroblasts isolated from the lung of wt and T-bet$^{-/-}$ mice.

may have a secondary role in the remodeling component of asthma induced by T-bet deficiency.

### *Fibroblasts isolated from T-bet$^{-/-}$ lung survive, proliferate more rapidly and secrete more TGF-β than wt lung fibroblasts*

Blockade of both IL-13 and IL-4 reduced TGF-β production in BALF and minimally in CD4+ cells suggesting that non-T cells were the source of the TGF-β detected. An attractive candidate cell type is the fibroblast itself. We isolated primary fibroblasts from lungs of T-bet$^{-/-}$ and wt mice. In several independent experiments, fibroblasts isolated from T-bet$^{-/-}$ lung were successfully cultured *in vitro* especially when IGF (25 ng ml$^{-1}$) was added to the culture medium. By contrast, under these conditions, fibroblasts isolated from wt littermates did not survive or grew slowly, assuming a spindle-shaped form before death (Fig. 7B and D). In addition, fibroblasts isolated from T-bet$^{-/-}$ mice were resistant to removal by trypsin treatment and could only be recovered by scraping. Microscopically, T-bet$^{-/-}$ fibroblasts were of rounded shape during logarithmic expansion at a time when they expressed vimentin (Fig. 7C and F). After reaching semi-confluence, their shape changed to an elongated or expanded form, and the cells acquired alpha smooth muscle filaments (Fig. 7E, G and I). To investigate the mechanism by which T-bet affects fibroblast behavior, semi-confluent fibroblasts were cultured overnight with low serum (0.4% FCS in DMEM) to reach cell synchronization. As shown in Fig. 7H, T-bet$^{-/-}$ lung fibroblasts spontaneously released increased amounts of TGF-β as compared with wt fibroblasts when cultured in the absence of serum (0.4%). T-bet transcripts are not present in lung fibroblasts and no T-bet protein can be detected in lung fibroblasts (data not shown). Thus, we assume that the microenvironment of the T-bet$^{-/-}$ lung, perhaps through autocrine feedback, results in a morphological and functional change in fibroblasts that is retained upon *in vitro* culture.

### *Blockade of TGF-β induces SMAD7 and reduces SMAD3 in lung fibroblasts and also diminishes lung fibrosis in vivo in T-bet$^{-/-}$ mice*

We next investigated the effect of TGF-β blockade in T-bet$^{-/-}$ lung fibroblasts. As shown in Fig. 8A, local blockade of TGF-β in T-bet$^{-/-}$ lung led to a down-regulation of vimentin, a marker of fibrosis. The expression of the inhibitory SMAD protein, SMAD7, is down-regulated at the basal state in T-bet$^{-/-}$ lung compared with wt littermates consistent with ongoing increased TGF-β signaling in these animals (Fig. 8B). As expected, anti-TGF-β treatment led to increased SMAD7 and decreased SMAD3 (Fig. 8C) expression in treated fibroblasts indicating an inhibition of TGF-β signaling in these cells.

## Discussion

$T_h2$ effectors cells develop from naive T cells under the influence of IL-4 produced by T and non-T cells such as IgE-activated mast cells and NK cells (36). It has been recently demonstrated that NKT cell-deficient mice do not develop AHR following antigen challenge and that this asthmatic phenotype can be reconstituted either by adoptive transfer of NKT cells producing IL-4 and IL-13 or by recombinant IL-13 alone which induces AHR through direct effects on airway smooth muscle cells (36). Since T-bet$^{-/-}$ mice possess very few NKT cells and those that are present are halted at an immature stage of differentiation (37), it is not likely that they are the origin of the asthmatic phenotype observed. IL-13

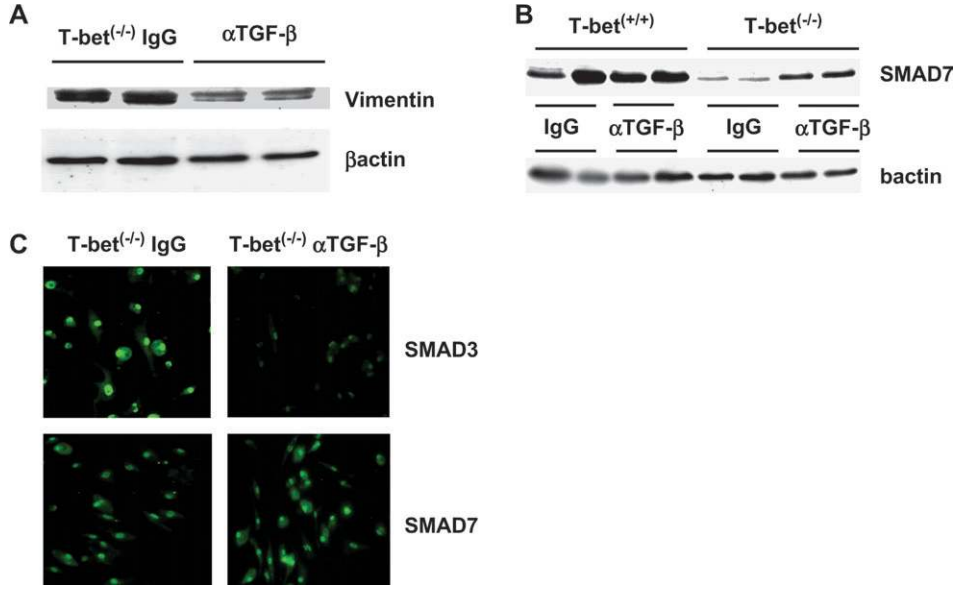


**Fig. 8.** Blockade of TGF-β induces SMAD7 and reduces SMAD3 in lung fibroblasts and also diminishes lung fibrosis *in vivo* in T-bet$^{-/-}$ mice. (A) Western blot analysis of lung proteins. Local blockade of TGF-β in T-bet$^{-/-}$ lung led to a down-regulation of vimentin, a marker of fibrosis. (B) Reverse transcription–PCR analysis reveals that expression of SMAD7 is down-regulated at the basal state in T-bet$^{-/-}$ lung compared with wt lung. (C) Immunofluorescence of T-bet$^{-/-}$ lung fibroblasts subjected to αTGF-β treatment leads to increased SMAD7 and decreased SMAD3 expression indicating an inhibition of TGF-β signaling.

shares 30% homology with IL-4 and appears to have certain overlapping biological activities in type II responses. Both cytokines use the IL-4R α-chain and the STAT6-dependent signal transduction pathway. However, despite some overlapping roles, these cytokines do have clearly distinct biological activities. IL-13 is a particularly important asthma-inducing cytokine as evidenced by the phenotype of mice that lack or over-express this gene as well as its abundant expression in human asthma (38–50). IL-13 over-production leads to airway hyperreactivity, mucus over-production, airway remodeling and most recently has been shown to be required for acidic mammalian chitinase-induced $T_h2$ inflammation and AHR in a aero-allergen model (1, 11, 12, 41, 44, 51–54). Our experiments show that blockade of IL-4 in the lung of T-bet-deficient mice affected only the inflammatory component of the asthmatic phenotype present in these mice. By contrast, blockade of IL-13 led to a down-regulation of AHR, inflammation and remodeling (see below).

TGF-β regulates many cellular processes including embryogenesis, inflammation, immune responses and tissue repair. Although TGF-β is released from degranulating platelets at the time of wounding, all of the participating cells can both produce and respond to TGF-β during the course of the healing process. TGF-β stimulates the chemotaxis of fibroblasts, neutrophils and macrophages within the wound bed, alters the pattern of cytokine production by macrophages and induces fibroblasts to secrete ECM proteins such as CLs and fibronectin. TGF-β inhibits the G(1)/S cell cycle transition and alters cytoskeletal organization through multiple parallel downstream signaling pathways. TGF-β signals through transmembrane receptor serine/threonine kinases that activate a family of cytoplasmic proteins called SMADs, which translocate to the nucleus to regulate expression of target genes (55–58). Although SMAD2 and SMAD3 are each phosphorylated directly by the TGF-β type I receptor kinase, SMAD3S plays a unique role in the cellular and tissue responses to wounding. Similarly, although both SMAD2 and SMAD3 are phosphorylated directly by the TGF-β and activin type I receptors (ALK5 and ALK4, respectively), selective DNA binding of SMAD3, and not SMAD2, likely directs their distinct cellular targets and different requirements in embryogenesis TGF-β-dependent synthesis of CLs 1, 3, 6 and 7 and tissue inhibitor of metalloproteinases-1 are SMAD3 dependent, as well as the more complex processes of TGF-β-dependent chemotaxis and inhibition of epithelial migration, implicating this pathway in both wound healing and fibrosis (55–60). We found evidence for a role of TGF-β signaling in inducing the chronic airway remodeling observed in T-bet$^{-/-}$ lung as evidenced by increased levels of vimentin, decreased expression of SMAD7 and increased expression of SMAD3 in the basal state. However, blockade of TGF-β signaling did not alter the AHR phenotype observed in these mice.

Blockade of IL-4 did not reduce vimentin expression indicating an exclusive function of IL-13 in induction of CL and fibrosis in the setting of T-bet deficiency. These results are consistent with other studies indicating that IL-4 failed to directly stimulate proliferation myofibroblast differentiation, and type I CL production in C57BL/6 murine lung fibroblasts, but was able to do so in CBA/J murine lung fibroblasts, albeit to a lesser extent than that observed with TGF-β, but with comparable intensity relative to the effects of IL-13 (33). However, lung fibroblasts from both murine strains were equally responsive to TGF-β and PDGF. Several pieces of evidence support the view that IL-4 is not directly responsible for induction of exaggerated ECM deposition but acts primarily as an indirect signal, possibly by regulating the expression of other more potent fibrogenic mediators. This concept is supported by recent studies demonstrating that IL-4 can increase TGF-β production (35). Our results are consistent with autocrine activation of fibroblasts in T-bet$^{-/-}$ lung stimulated by release of IL-13 and IL-4 from CD4+ lung cells. Further, consistent with the present data, there are reports in the literature showing SMAD3 mediated auto-induction of TGF-β (58) in activated fibroblasts. Compared with fibroblasts derived from wt mice, SMAD3$^{-/-}$ fibroblasts showed reduced *in vitro* proliferative and profibrotic responses to TGF-β (59).

Mice with a targeted deletion of the T-bet gene spontaneously develop AHR, airway inflammation and increased production of type II cytokines from BALF. They also display airway remodeling as evidenced by increased deposition of CL type III around the airways and by transformation of fibroblasts into myofibroblasts. This constellation of features resembles what is seen in the human disease where the airways of asthmatic patients are occupied by $T_h2$-type CD4 cells producing IL-13, IL-4 and IL-5 that contribute to lung eosinophilia (IL-5), hyperresponsiveness (IL-13) and fibrosis (IL-4, IL-13). Here we have investigated the mechanisms by which T-bet deficiency leads to an asthmatic phenotype. Our experiments suggest a scenario in which T-bet deficiency results in over-production of IL-13 by $T_h2$ cells which in turn leads to over-production of IL-5 and of the profibrotic cytokine TGF-β. However, IL-13 acts independently of TGF-β in eliciting the AHR observed in the absence of T-bet. It is interesting that T-box family members have been reported to be responsive to mesoderm/inducing proteins, such as activin, a member of the TGF-β family and basic fibroblast growth factor (15). We and others have previously reported a negative feedback loop wherein TGF-β itself down-regulates the expression of T-bet which in turn represses the production of TGF-β (16, 20). We have also recently discovered polymorphisms in the T-bet locus that correlate with the asthmatic phenotype (61); polymorphisms in the IL-13 gene have been identified that correlate with asthma and allergy in a Dutch population (17, 42) and a TGF-β1 polymorphism C509T has been shown to be associated with asthma (62). One can envision a scenario in the asthmatic lung whereby individuals with genetically lower levels or activity of T-bet (or increased levels or activity of TGF-β or IL-13) instigate a negative feedback loop resulting in IL-13-dependent TGF-β over-production and consequent airway remodeling in the setting of other predisposing genetic and environmental stimuli. Increasing the activity of T-bet in the setting of the asthmatic phenotype may prove an effective immunotherapeutic strategy.

**Acknowledgements**

The authors thank M. Schipp, C. Lux and P. Scholtes for excellent technical assistance and L. de Elizalde for expert manuscript preparation. This work was supported by an SFB 548-B8 (S.F.) and NIH grant AI31541 (L.H.G.).

## Abbreviations

| | |
|---|---|
| AHR | airway hyperresponsiveness |
| αSMA | alpha smooth muscle actin |
| BALF | bronchoalveolar lavage fluid |
| ECM | extracellular matrix |
| i.n. | intra-nasally |
| i.p. | intra-peritoneal |
| OVA | ovalbumin peptide |
| TGF-β | transforming growth factor beta |
| Treg | T regulatory cell |
| TBS | Tris-buffered saline |
| wt | wild-type |

## References


1 Cohn, L., Elias, J. A. and Chupp, G. L. 2004. Asthma: mechanisms of disease persistence and progression. *Annu. Rev. Immunol.* 22:789.

2 Gavett, S. H., O'Hearn, D. J., Li, X., Huang, S. K., Finkelman, F. D. and Wills-Karp, M. 1995. Interleukin 12 inhibits antigen-induced airway hyperresponsiveness, inflammation, and Th2 cytokine expression in mice. *J. Exp. Med.* 182:1527.

3 Szabo, S. J., Sullivan, B. M., Stemmann, C., Satoskar, A. R., Sleckman, B. P. and Glimcher, L. H. 2002. Distinct effects of T-bet in Th1 lineage commitment and IFN-γ production in CD4 and CD8 T cells. *Science* 295:338.

4 Szabo, S. J., Sullivan, B. M., Peng, S. L. and Glimcher, L. H. 2003. Molecular mechanisms regulating Th1 immune responses. *Annu. Rev. Immunol.* 21:713.

5 Finotto, S., Neurath, M. F., Glickman, J. N. *et al.* 2002. Development of spontaneous airway changes consistent with human asthma in mice lacking T-bet. *Science* 295:336.

6 Finotto, S. and Glimcher, L. H. 2004. T cell directives for transcriptional regulation in asthma. *Springer Semin. Immunopathol.* 25:281.

7 Simmons, J. G., Pucilowska, J. B., Keku, T. O. and Lund, P. K. 2002. IGF-I and TGF-beta1 have distinct effects on phenotype and proliferation of intestinal fibroblasts. *Am. J. Physiol. Gastrointest. Liver Physiol.* 283:G809.

8 Richter, A., Puddicombe, S. M., Lordan, J. L. *et al.* 2001. The contribution of interleukin (IL)-4 and IL-13 to the epithelial-mesenchymal trophic unit in asthma. *Am. J. Respir. Cell Mol. Biol.* 25:385.

9 Doucet, C., Brouty-Boye, D., Pottin-Clemenceau, C., Canonica, G. W., Jasmin, C. and Azzarone, B. 1998. Interleukin (IL) 4 and IL-13 act on human lung fibroblasts. Implication in asthma. *J. Clin. Invest.* 101:2129.

10 Zhu, Z., Enhorning, G., Zheng, T. *et al.* 2003. Interleukin-13 induces surfactant function abnormality in the murine lung. *Chest* 123:375S.

11 Zhu, Z., Zheng, T., Homer, R. J. *et al.* 2004. Acidic mammalian chitinase in asthmatic Th2 inflammation and IL-13 pathway activation. *Science* 304:1678.

12 Lee, C. G., Homer, R. J., Zhu, Z. *et al.* 2001. Interleukin-13 induces tissue fibrosis by selectively stimulating and activating transforming growth factor β. *J. Exp. Med.* 194:809.

13 Robinson, D. S. and Lloyd, C. M. 2002. Asthma: T-bet- a master controller? *Curr. Biol.* 12:R322.

14 Finotto, S., De Sanctis, G. T., Lehr, H. A. *et al.* 2001. Treatment of allergic airway inflammation and hyperresponsiveness by antisense-induced local blockade of gata-3 expression. *J. Exp. Med.* 193:1247.

15 Packham, E. A. and Brook, J. D. 2003. T-box genes in human disorders. *Hum. Mol. Genet.* 12(Spec. no. 1):R37.

16 Gorelik, L., Constant, S. and Flavell, R. A. 2002. Mechanism of transforming growth factor β-induced inhibition of T helper type 1 differentiation. *J. Exp. Med.* 195:1499.

17 Howard, T. D., Whittaker, P. A., Zaiman, A. L. *et al.* 2001. Identification and association of polymorphisms in the interleukin-13 gene with asthma and atopy in a Dutch population. *Am. J. Respir. Cell Mol. Biol.* 25:377.

18 Finotto, S., Buerke, M., Lingnau, K., Schmitt, E., Galle, P. R. and Neurath, M. F. 2001. Local administration of antisense phosphorothioate oligonucleotides to the c-kit ligand, stem cell factor, suppresses airway inflammation and IL-4 production in a murine model of asthma. *J. Allergy Clin. Immunol.* 107:279.

19 Akbari, O., Stock, P., DeKruyff, R. H. and Umetsu, D. T. 2003. Role of regulatory T cells in allergy and asthma. *Curr. Opin. Immunol.* 15:627.

20 Neurath, M. F., Weigmann, B., Finotto, S. *et al.* 2002. The transcription factor T-bet regulates mucosal T cell activation in experimental colitis and Crohn's disease. *J. Exp. Med.* 195:1129.

21 Stassen, M., Jonuleit, H., Muller, C. *et al.* 2004. Differential regulatory capacity of CD25+ T regulatory cells and preactivated CD25+ T regulatory cells on development, functional activation, and proliferation of Th2 cells. *J. Immunol.* 173:267.

22 Szabo, S. J., Kim, S. T., Costa, G. L., Zhang, X., Fathman, G. C. and Glimcher, L. H. 2000. A novel transcription factor, T-bet, directs Th1 lineage commitment. *Cell* 100:655.

23 Avni, O., Lee, D., Macian, F., Szabo, S. J., Glimcher, L. H. and Rao, A. 2002. Th cell differentiation is accompanied by dynamic changes in histone acetylation of cytokine genes. *Nat. Immunol.* 3:643.

24 Mullen, A. C., Hutchins, A. S., High, F. A. *et al.* 2002. Hlx is induced by and genetically interacts with T-bet to promote heritable Th1 gene induction. *Nat. Immunol.* 10:652.

25 Afkarian, M., Sedy, J. R., Yang, J. *et al.* 2002. T-bet is a STAT1-induced regulator of IL-12R expression in naive CD4+ T cells. *Nat. Immunol.* 3:549.

26 Lighvani, A. A., Frucht, D. M., Jankovic, D. *et al.* 2001. T-bet is rapidly induced by interferon-γ in lymphoid and myeloid cells. *Proc. Natl Acad. Sci. USA* 98:15137.

27 Mullen, A. C., High, F. A., Hutchins, A. S. *et al.* 2001. Role of T-bet in commitment of TH1 cells before IL-12-dependent selection. *Science* 292:1907.

28 Ohno, I., Nitta, Y., Yamauchi, K. *et al.* 1996. Transforming growth factor beta 1 (TGF beta 1) gene expression by eosinophils in asthmatic airway inflammation. *Am. J. Respir. Cell Mol. Biol.* 15:404.

29 Minshall, E. M., Leung, D. Y., Martin, R. J. *et al.* 1997. Eosinophil-associated TGF-beta1 mRNA expression and airways fibrosis in bronchial asthma. *Am. J. Respir. Cell Mol. Biol.* 17:326.

30 Khalil, N., Parekh, T. V., O'Connor, R. *et al.* 2001. Regulation of the effects of TGF-beta 1 by activation of latent TGF-beta 1 and differential expression of TGF-beta receptors (T beta R-I and T beta R-II) in idiopathic pulmonary fibrosis. *Thorax* 56:907.

31 Martin, M., Lefaix, J. and Delanian, S. 2000. TGF-beta1 and radiation fibrosis: a master switch and a specific therapeutic target? *Int. J. Radiat. Oncol. Biol. Phys.* 47:277.

32 Roberts, A. B., Piek, E., Bottinger, E. P., Ashcroft, G., Mitchell, J. B. and Flanders, K. C. 2001. Is SMAD3 a major player in signal transduction pathways leading to fibrogenesis? *Chest* 120:43S.

33 Huaux, F., Liu, T., McGarry, B., Ullenbruch, M. and Phan, S. H. 2003. Dual roles of IL-4 in lung injury and fibrosis. *J. Immunol.* 170:2083.

34 Kolodsick, J. E., Toews, G. B., Jakubzick, C. *et al.* 2004. Protection from fluorescein isothiocyanate-induced fibrosis in IL-13-deficient, but not IL-4-deficient, mice results from impaired collagen synthesis by fibroblasts. *J. Immunol.* 172:4068.

35 Kodera, T., McGaha, T. L., Phelps, R., Paul, W. E. and Bona, C. A. 2002. Disrupting the IL-4 gene rescues mice homozygous for the tight-skin mutation from embryonic death and diminishes TGF-beta production by fibroblasts. *Proc. Natl Acad. Sci. USA* 99:3800.

36 Akbari, O., Stock, P., Meyer, E. *et al.* 2003. Essential role of NKT cells producing IL-4 and IL-13 in the development of allergen-induced airway hyperreactivity. *Nat. Med.* 9:582.

37 Townsend, M., Weinmann, A. S., Matsuda, J. *et al.* 2004. T-bet regulates the terminal maturation and homeostasis of NK and Val4iNKT cells. *Immunity* 20:477.

38 Wills-Karp, M., Luyimbazi, J., Xu, X. *et al.* 1998. Interleukin-13: central mediator of allergic asthma. *Science* 282:2258.

39 Walter, D. M., McIntire, J. J., Berry, G. *et al.* 2001. Critical role for IL-13 in the development of allergen-induced airway hyperreactivity. *J. Immunol.* 167:4668.

40 Mattes, J., Yang, M., Mahalingam, S. *et al.* 2002. Intrinsic defect in T cell production of interleukin (IL)-13 in the absence of both IL-5 and eotaxin precludes the development of eosinophilia and airways hyperreactivity in experimental asthma. *J. Exp. Med.* 195:1433.
41 Kuperman, D. A., Huang, X., Koth, L. L. *et al.* 2002. Direct effects of interleukin-13 on epithelial cells cause airway hyperreactivity and mucus overproduction in asthma. *Nat. Med.* 8:885.
42 Wills-Karp, M. 2000. The gene encoding interleukin-13: a susceptibility locus for asthma and related traits. *Respir. Res.* 1:19.
43 Wills-Karp, M. 2001. IL-12/IL-13 axis in allergic asthma. *J. Allergy Clin. Immunol.* 107:9.
44 Zhu, Z., Homer, R. J., Wang, Z. *et al.* 1999. Pulmonary expression of interleukin-13 causes inflammation, mucus hypersecretion, subepithelial fibrosis, physiologic abnormalities, and eotaxin production. *J. Clin. Invest.* 103:779.
45 Wenzel, S. E., Trudeau, J. B., Barnes, S. *et al.* 2002. TGF-beta and IL-13 synergistically increase eotaxin-1 production in human airway fibroblasts. *J. Immunol.* 169:4613.
46 Foster, P. S., Martinez-Moczygemba, M., Huston, D. P. and Corry, D. B. 2002. Interleukins-4, -5, and -13: emerging therapeutic targets in allergic disease. *Pharmacol. Ther.* 94:253.
47 Kumar, R. K., Herbert, C., Yang, M., Koskinen, A. M., McKenzie, A. N. and Foster, P. S. 2002. Role of interleukin-13 in eosinophil accumulation and airway remodelling in a mouse model of chronic asthma. *Clin. Exp. Allergy* 32:1104.
48 Schmid-Grendelmeier, P., Altznauer, F., Fischer, B. *et al.* 2002. Eosinophils express functional IL-13 in eosinophilic inflammatory diseases. *J. Immunol.* 169:1021.
49 Grunig, G., Ford, J. G., Donaldson, D. D. *et al.* 2002. Roles of interleukin-13 and interferon-gamma in lung inflammation. *Chest* 121:88S.
50 Mattes, J., Yang, M., Siqueira, A. *et al.* 2001. IL-13 induces airways hyperreactivity independently of the IL-4R alpha chain in the allergic lung. *J. Immunol.* 167:1683.
51 Zheng, T., Zhu, Z., Liu, W. *et al.* 2003. Cytokine regulation of IL-13Ralpha2 and IL-13Ralpha1 *in vivo* and *in vitro*. *J. Allergy Clin. Immunol.* 111:720.
52 Taube, C., Duez, C., Cui, Z. H. *et al.* 2002. The role of IL-13 in established allergic airway disease. *J. Immunol.* 169:6482.
53 Wood, N., Whitters, M. J., Jacobson, B. A. *et al.* 2003. Enhanced interleukin (IL)-13 responses in mice lacking IL-13 receptor alpha 2. *J. Exp. Med.* 197:703.
54 McKenzie, A. N. and Fallon, P. G. 2003. Decoy receptors in the regulation of T helper cell type 2 responses. *J. Exp. Med.* 197:675.
55 Funaba, M. and Mathews, L. S. 2000. Identification and characterization of constitutively active Smad2 mutants: evaluation of formation of Smad complex and subcellular distribution. *Mol. Endocrinol.* 14:1583.
56 Souchelnytskyi, S., Tamaki, K., Engstrom, U., Wernstedt, C., ten Dijke, P. and Heldin, C. H. 1997. Phosphorylation of Ser465 and Ser467 in the C terminus of Smad2 mediates interaction with Smad4 and is required for transforming growth factor-beta signaling. *J. Biol. Chem.* 272:28107.
57 Kretzschmar, M., Doody, J., Timokhina, I. and Massague, J. 1999. A mechanism of repression of TGFβ/Smad signaling by oncogenic Ras. *Genes Dev.* 13:804.
58 Piek, E., Ju, W. J., Heyer, J. *et al.* 2001. Functional characterization of transforming growth factor beta signaling in Smad2- and SMAD3-deficient fibroblasts. *J. Biol. Chem.* 276:19945.
59 Lakos, G., Takagawa, S., Chen, S. J. *et al.* 2004. Targeted disruption of TGF-beta/SMAD3 signaling modulates skin fibrosis in a mouse model of scleroderma. *Am. J. Pathol.* 165:203.
60 Flanders, K. C., Major, C. D., Arabshahi, A. *et al.* 2003. Interference with transforming growth factor-beta/ SMAD3 signaling results in accelerated healing of wounds in previously irradiated skin. *Am. J. Pathol.* 163:2247.
61 Tantisira, K. G., Hwang, E. S., Raby, B. A. *et al.* 2004. TBX21: a functional variant predicts improvement in asthma with the use of inhaled corticosteroids. *Proc. Natl Acad. Sci. USA* 101: 18099.
62 Silverman, E. S., Palmer, L. J., Subramaniam, V. *et al.* 2004. Transforming growth factor-beta1 promoter polymorphism C-509T is associated with asthma. *Am. J. Respir. Crit. Care Med.* 169:214.